Cell Reports Medicine, Volume *4*

Supplemental information

Preclinical development of a chimeric antigen receptor T cell therapy targeting FGFR4 in rhabdomyosarcoma

Meijie Tian, Jun S. Wei, Nityashree Shivaprasad, Steven L. Highfill, Berkley E. Gryder, David Milewski, G. Tom Brown, Larry Moses, Hannah Song, Jerry T. Wu, Peter Azorsa, Jeetendra Kumar, Dina Schneider, Hsien-Chao Chou, Young K. Song, Abdelrahman Rahmy, Katherine E. Masih, Yong Yean Kim, Brian Belyea, Corinne M. Linardic, Boro Dropulic, Peter M. Sullivan, Poul H. Sorensen, Dimiter S. Dimitrov, John M. Maris, Crystal L. Mackall, Rimas J. Orentas, Adam T. Cheuk, and Javed Khan

Supplementary information

Preclinical development of a Chimeric Antigen Receptor T-cell therapy targeting FGFR4 in rhabdomyosarcoma

Meijie Tian, Jun S. Wei, Nityashree Shivaprasad, Steven L. Highfill, Berkley E. Gryder, David Milewski, G Tom Brown, Larry Moses, Hannah Song, Jerry T. Wu, Peter Azorsa, Jeetendra Kumar, Dina Schneider, Hsien-Chao Chou, Young K. Song, Abdelrahman Rahmy, Katherine E. Masih, Yong Yean Kim, Brian Belyea, Corinne M. Linardic, Boro Dropulic, Peter M. Sullivan, Poul H. Sorensen, Dimiter S. Dimitrov, John M. Maris, Crystal L. Mackall, Rimas J. Orentas, Adam T. Cheuk, and Javed Khan

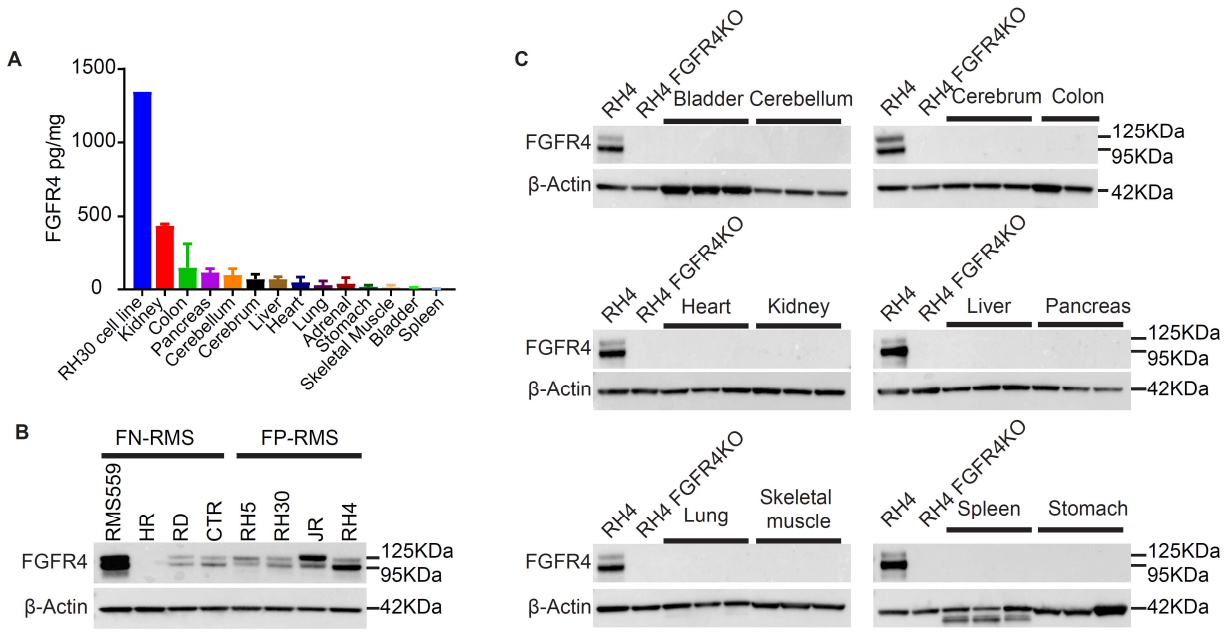

Figure S1. Protein expression of FGFR4 in RMS cell lines and normal organs. Related to Figure 1. (A) FGFR4 protein is expressed at lower levels in normal tissues by electrochemiluminescence assay compared to the positive control FP-RMS cell line RH30. **(B)** FGFR4 protein is expressed in FP-RMS and some FN-RMS cell lines by Western. **(C)** FGFR4 expression is only detected in RH30 but not in normal tissues.

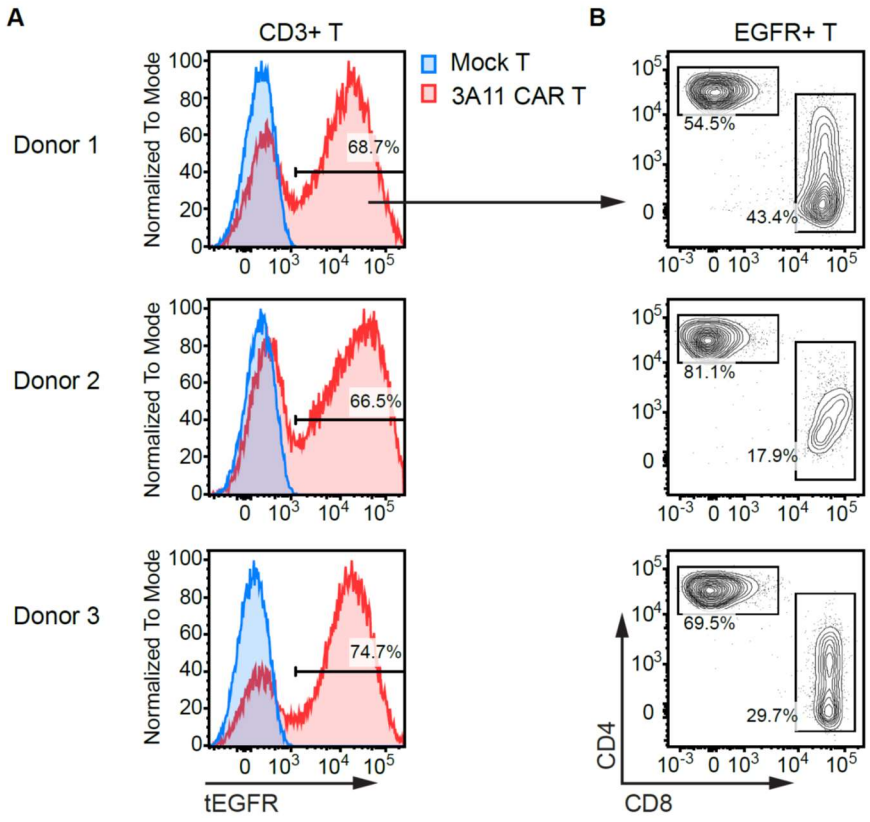

Figure S2. Transduction efficiency of 3A11 CAR T-cells manufactured using the CliniMACS® Prodigy system from three healthy donors. Related to Figure 4. (A) Representative flow cytometry plots show the transduction efficiency of 3A11 CAR T-cells by staining with EGFR antibody. **(B)** The percentages of $CD4^+$ or $CD8^+$ CAR T-cells gating on the $EGFR^+$ T-cells are shown.

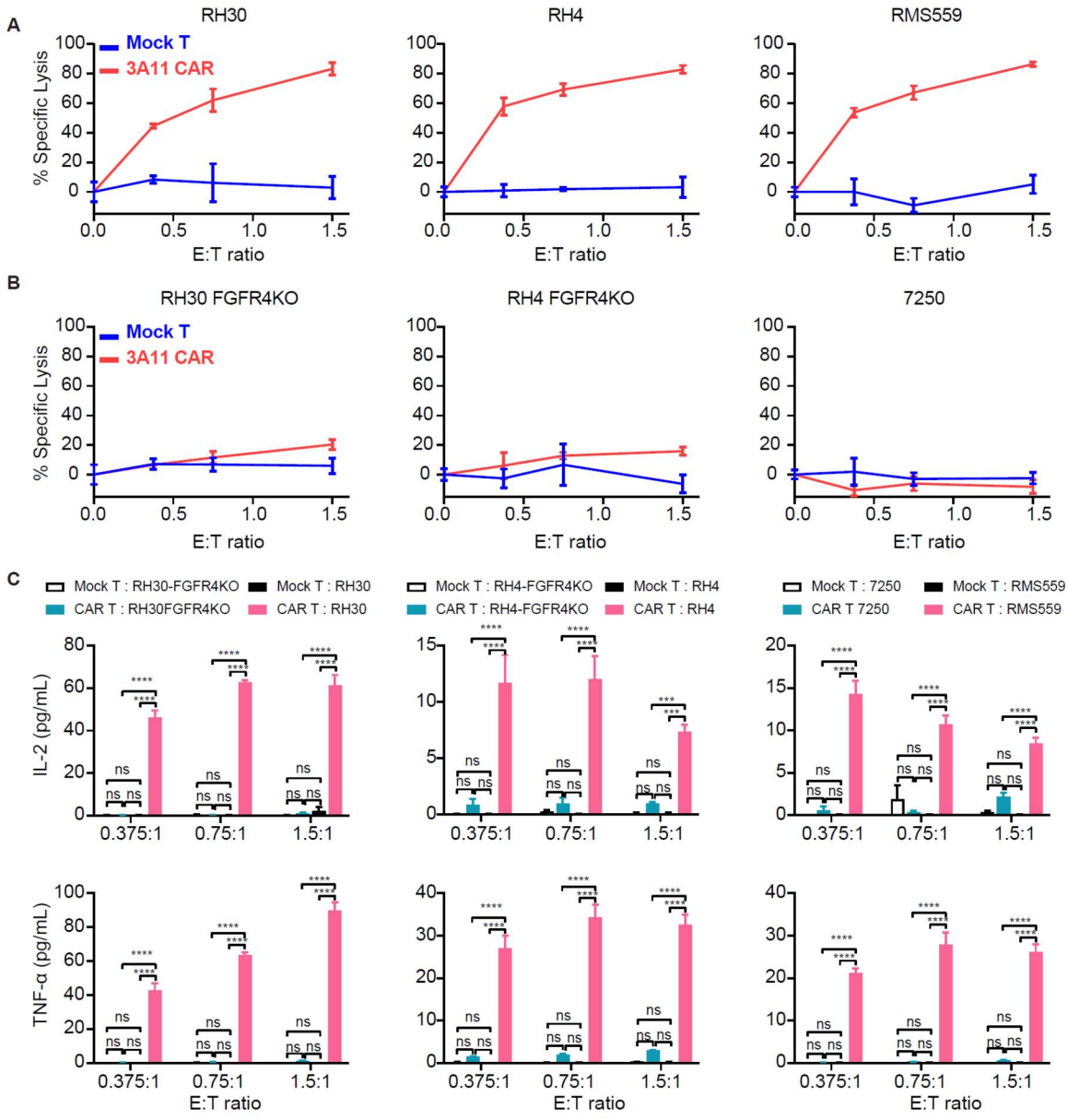

Figure S3. 3A11 CAR T-cells show specific killing activity to FGFR4 expressing RMS tumor cells. Related to Figure 4. (**A** and **B**) The specific lysis percentage of 3A11 CAR T-cells co-cultured with FGFR4 expressing RMS cells (**A**) or with RH30 FGFR4-KO, RH4 FGFR4-KO or human fibroblast cell line 7250 (**B**) at the indicated E:T ratios in an RTCA. (**C**) IL-2 and TNF-α production levels of 3A11 CAR T-cells following a 20-hour co-culture with FGFR4 expressing RMS cells or FGFR4-KO or 7250 are shown. Values represent mean ± SEM. Statistical test represents two-way ANOVA multiple comparisons (****$p < 0.0001$, ***$p < 0.01$, **$p < 0.01$, *$p < 0.05$; ns, $p > 0.05$).

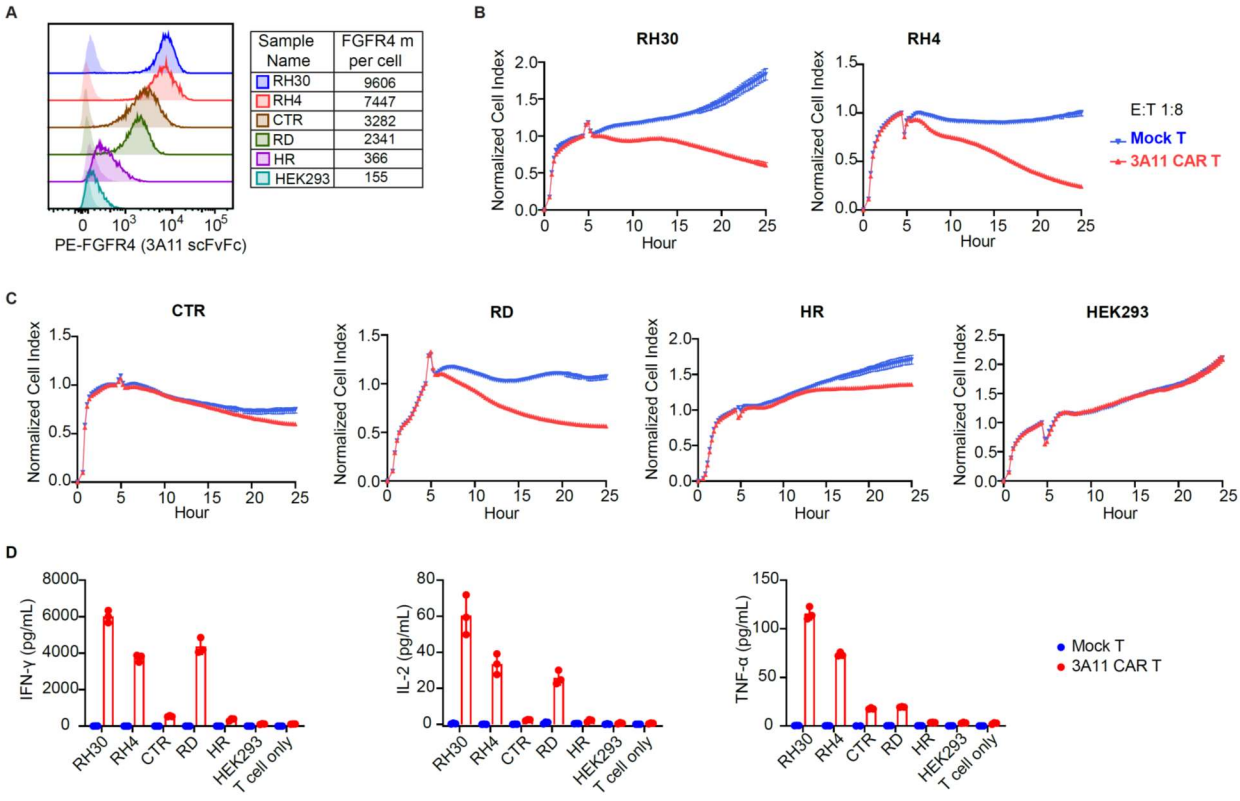

Figure S4. 3A11 CAR T-cells exhibited low/absent antitumor activity when co-culturing with cells expressing low levels of FGFR4, such as HR or HEK293 cells. Related to Figure 5. (A) Representative flow cytometry plot showing differential levels of FGFR4 expression on RMS cell lines and normal cell HEK293. And Surface FGFR4 molecule numbers/cell of indicated cell lines listed in the right table are estimated and quantified by PE quantitation beads. (B and C) Cytotoxicity assays show the differential killing activity of 3A11 CAR T-cells to different RMS cell lines or HEK293 with variable FGFR4 expression levels at an E:T ratio of 1:8. (D) Cytokine release assays show 3A11 CAR T-cells only release high-level cytokine when co-cultured with RH30, RH4, or RD cells, rather than the CTR, HR, or HEK293 cells. These data are consistent with their killing ability. Values in (B) and (C) represents mean ± SEM. Values in (D)represents mean ± SD. Representative of $n = 2$ independent experiments with $n = 2$ individual donors.

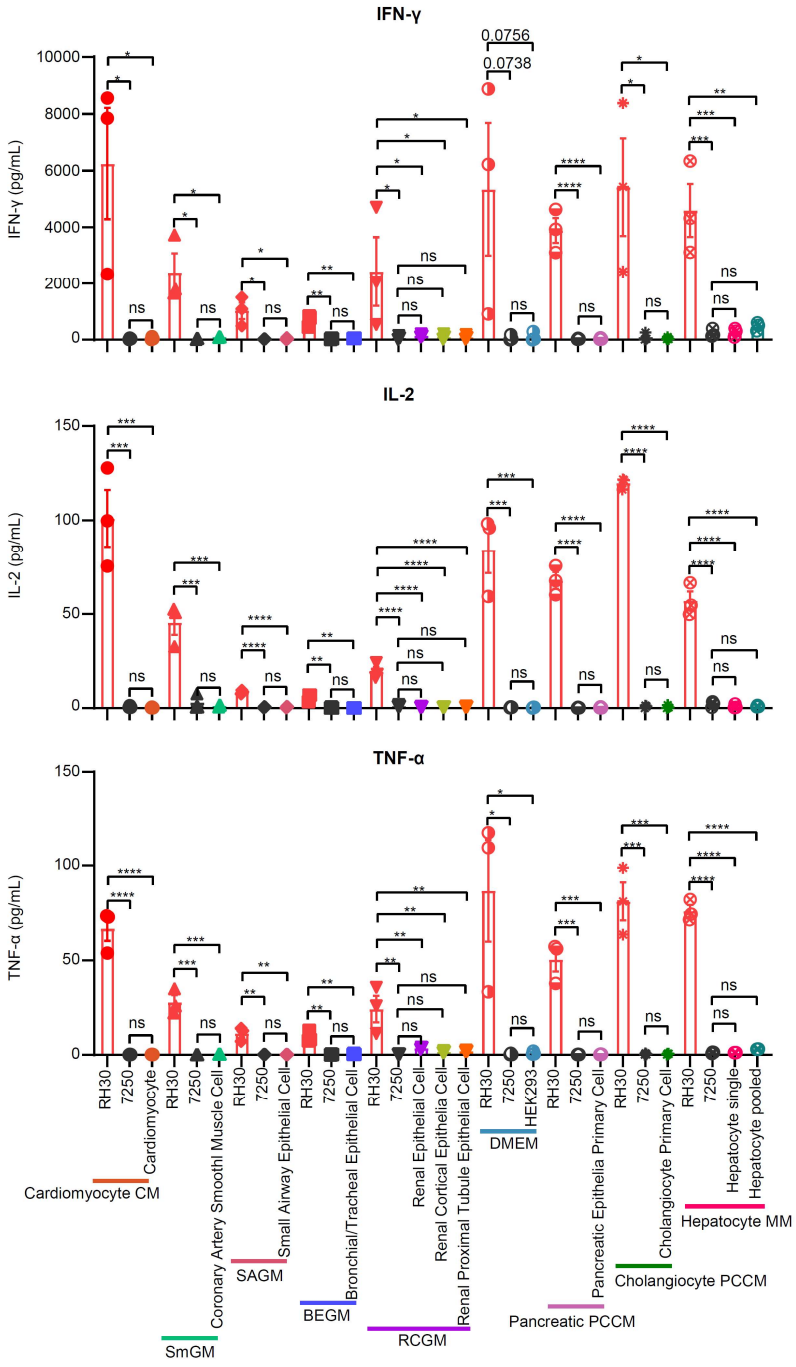

Figure S5. 3A11 CAR T-cells exhibited similar low cytokine production when co-culturing with primary cells as 7250 cells. Related to Figure 5. Cytokine (IFN-γ, IL-2, or TNF-α) released by FGFR4 CAR T-cells from three individual donors when coculturing with primary cells or the FGFR4 negative cell line 7250, compared to the positive cell RH30, grown in their respective media. Statistics represent ordinary one-way ANOVA (****$p < 0.0001$, ***$p < 0.01$, **$p < 0.01$, *$p < 0.05$; ns, $p > 0.05$). Values show $n = 3$ independent experiments with $n = 3$ individual donors.

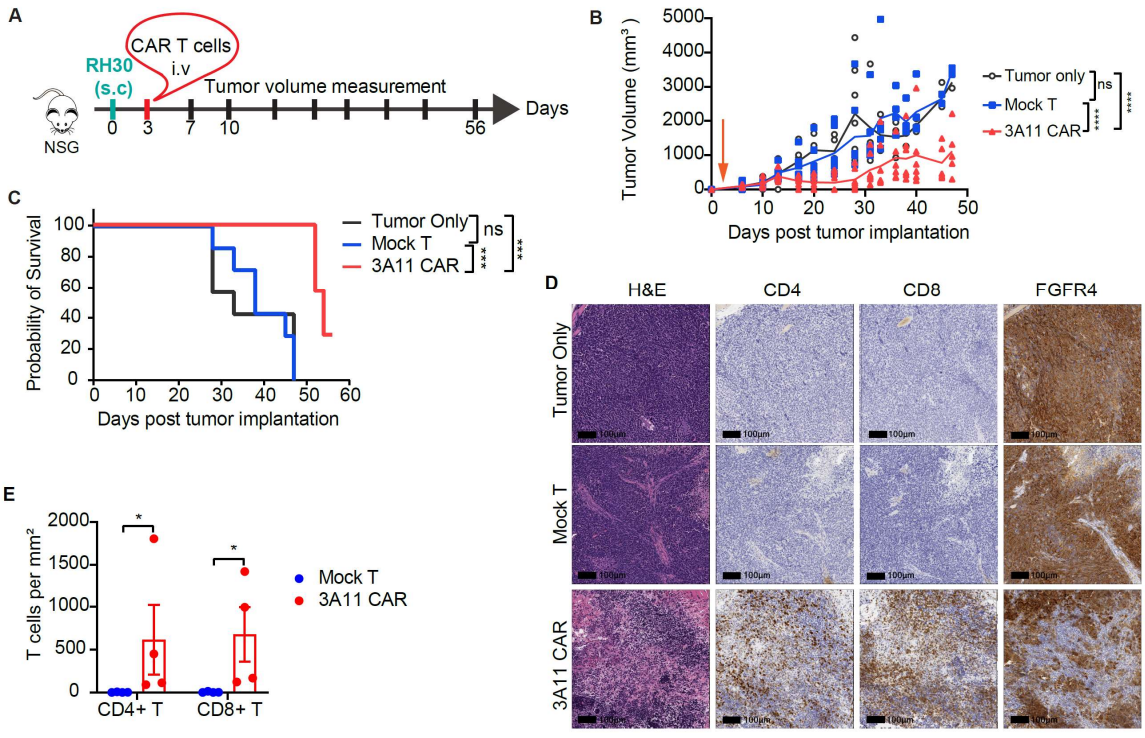

Figure S6. 3A11 CAR T-cells successfully infiltrate into a solid subcutaneous RMS tumor. Related to Figure 7. (**A**) Schema of the RH30 subcutaneous xenograft model infused with HBSS vehicle, mock or 3E6 CAR T-cells on day 3 post tumor inoculation. (**B**) Individual RH30 tumor volume after receiving mock or CAR T-cells treatment was measured by caliper. Arrow indicated the day that mice received treatment. Means and each replicate are shown, n = 7. Mixed-effects analysis is used to calculate the p values between each two groups individually. ****$p < 0.0001$. (**C**) Kaplan-Meier survival analysis of mice receiving different treatments are shown. Tumor only vs 3A11 CAR ***p = 0.0003; for mock T vs 3A11 CAR ***p = 0.0002. (**D**) Representative images of H&E, IHC staining within RH30 tumor grafts from mice treated with HBSS, mock T-cells and 3A11 CAR T-cells individually. All tumors are intensely positive for FGFR4. 3A11 CAR T-cells treated mice typically harbor small tumors that contain significant CD4 and CD8 positive tumor infiltrating lymphocytes. Rare CD4 and CD8 positive cells are observed in mock T-cell treated tumors. Scale bars labeled on image is 100µm, n = 4. (**E**) $CD4^+$ or $CD8^+$ T-cells significantly infiltrating into tumors treated with 3A11 CAR T-cells. Annotations were made to include tumor tissue and exclude tumor necrosis and section artifact for quantification of IHC. Digital pathology for biomarker quantification was performed following Whole Slide Imaging (WSI). Thresholds for positivity was determined using known positive controls. $CD4^+$ and $CD8^+$ T-cells are reported as number of positive cells per mm^2 of slide area. Mann-Whitney test was used to calculate the p value. * $p < 0.05$.

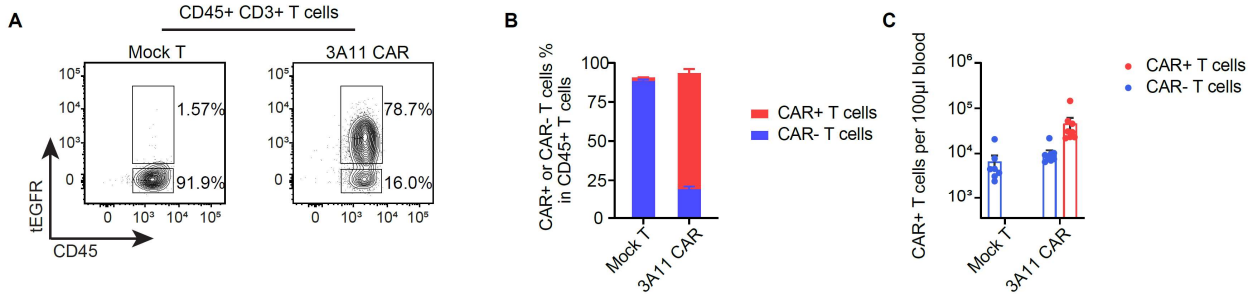

Figure S7. 3A11 CAR T-cells phenotype in RH4 orthotopic tumor model. Related to Figure 7. (A) Representative flow cytometric plots of CAR T-cell percentages in $CD45^+$ $CD3^+$ T-cells of blood collected from above mice at day 49 post RH4 implant. (B and C) Percentage of CAR^+ and CAR^- in $CD45^+$ $CD3^+$ T-cells from PBMCs (B) and total counts of the indicated T-cells in 100µl blood (C). Data are shown as the mean ± SEM (*n* = 7 or 8).